EUROPEAN ORGANIZATION FOR NUCLEAR RESEARCH

CERN-EP/87-16
26 January 1987

CORRELATIONS BETWEEN THE PRODUCTION OF PROMPT POSITRONS AT LOW TRANSVERSE MOMENTUM AND THE ASSOCIATED CHARGED MULTIPLICITY

(The Axial Field Spectrometer Collaboration)

T. Åkesson[4], M.G. Albrow[12], S. Almehed[8], E. Anassontzis[1], R. Batley[4], O. Benary[13], H. Boggild[5], O. Botner[5], H. Breuker[4], V. Burkert[2], R. Carosi[4], V. Chernyatin[9], Y. Choi[11], W.E. Cleland[11], S. Dagan[13], E. Dahl-Jensen[5], I. Dahl-Jensen[5], G. Damgaard[5], B. Dolgoshein[9], S. Eidelman[10], C.W. Fabjan[4], I. Gavrilenko[7], U. Goerlach[4], K.H. Hansen[5], V. Hedberg[8], G. Jarlskog[8], A. Kalinovsky[9], V. Kanteserov[9], S. Katsanevas[4], C. Kourkoumelis[1], R. Kroeger[11], K. Kulka[8], D. Lissauer[13], B. Lörstad[8], I. Mannelli[4], A. Markou[1], S. Mayburov[7], N.A. McCubbin[12], U. Mjörnmark[8], R. Møller[5], P. Nevsky[9], B.S. Nielsen[4], L.H. Olsen[4], Y. Oren[13], L.K. Resvanis[1], J. Schukraft[4], A. Shmeleva[7], H. Specht[6], I. Stumer[3], M. Sullivan[11], H.H. Thodberg[5], J.A. Thompson[11], J. Williamson[12], W.J. Willis[4] and M. Winik[3]

ABSTRACT

The production of prompt positrons in pp collisions at $\sqrt{s}$ = 63 GeV and y = 0 has been measured as a function of the associated charged-particle multiplicity over the p_T interval $0.12 < p_T < 1.0$ GeV/c. The results indicate that the production of positrons is proportional to the square of the mean multiplicity at low p_T (< 0.4 GeV/c). Such a quadratic dependence is not expected from final-state sources such as hadronic bremsstrahlung or hadronic decays. It could, however, indicate a production mechanism of the soft lepton continuum over an extended volume during the early stages of the collision.

(Submitted to Physics Letters B)

1 University of Athens, Greece.
2 Physikalisches Institut, Universität Bonn, Fed. Rep. Germany.
3 Brookhaven National Laboratory, Upton, NY, USA.
4 CERN, Geneva, Switzerland.
5 Niels Bohr Institute, University of Copenhagen, Denmark.
6 Physikalisches Institut, University of Heidelberg, Fed. Rep. Germany.
7 Lebedev Institute, Moscow, USSR.
8 University of Lund, Sweden.
9 Moscow Physical Engineering Institute, Moscow, USSR.
10 Novosibirsk Institute of Nuclear Physics, Novosibirsk, USSR.
11 University of Pittsburgh, Pa., USA.
12 Rutherford Appleton Laboratory, Didcot, UK.
13 University of Tel Aviv, Israel.

1. INTRODUCTION

We have recently reported observations of a strong increase up to ~ 10^{-3} of the electron-to-pion ratio at low transverse momentum [1]. This measurement was in agreement with other ISR experiments [2], which at somewhat higher p_T had noticed a production of prompt electrons that could not be fully attributed to known sources such as hadronic bremsstrahlung or the decay of charmed particles. Other non-ISR experiments at lower $\sqrt{s}$ have also seen an excess of electrons above known sources at low p_T [3]; however, the subject has been somewhat controversial [4].

Studies of low-mass dilepton production have led to the discovery of a dilepton continuum with masses $m < 0.6$ GeV/c^2, i.e. below the ϱ^0 and ω. This dilepton continuum has been seen both in e^+e^- [5] and $\mu^+\mu^-$ channels [6]. The production rate of these pairs is up to two orders of magnitude larger than what would be expected from the Drell–Yan process. It is conceivable that the strong increase of the e^+/π ratio at low p_T is solely due to this low mass e^+e^- continuum.

So far the low-mass pair continuum has not been very well understood. One of the proposed explanations for the production of these low-mass lepton pairs is the so-called soft-annihilation model [7]. The basic idea of this model was originally proposed by Bjorken and Weisberg [8]. In the soft-annihilation model, low-mass lepton pairs are created through annihilation of quarks and antiquarks **produced** during the hadronic collision. It has been suggested [9] that the cross-section for the production of e^+e^- pairs according to this model should be proportional to the square of the particle density. Similar models such as the thermodynamic models [10] give the same variation with particle density [11].

Here we report on a study of the central production of prompt positrons as a function of the associated charged-particle multiplicity in the rapidity region $|y| < 1$. We observe a significant difference between the multiplicity dependence of the low p_T positrons, which could originate from the low-mass pair continuum, and the high-p_T positrons, which are attributed mainly to the decay of charmed particles.

2. APPARATUS

The experiment was performed at the Axial Field Spectrometer (AFS) [12] at the CERN Intersecting Storage Rings (ISR), with the configuration shown in fig. 1. An efficient electron identification was obtained already at the trigger level by two gas Cherenkov counters, filled with CO_2 at atmospheric pressure. Two scintillation counters positioned behind the Cherenkovs were also used in the trigger system. To allow for time-of-flight identification, and in order to reduce the pile-up in the Cherenkov detectors, one of the uranium calorimeter walls was retracted to a distance of 5 m from the intersection. However, the normal 2π azimuthal coverage of the calorimeter was reduced to $^3/_2\ \pi$ because of the retracted wall. The rapidity coverage of the remaining three calorimeter walls in the centre of mass varied with azimuth from $|y| < 0.7$ to $|y| < 1.2$. Of the two highly segmented NaI-crystal walls only that behind the Cherenkov counters was used for electron-identification and trigger purposes.

The charged tracks were detected by the central vertex detector, a cylindrical drift chamber 1.40 m long with azimuthal segmentation of 4° sectors and a rapidity coverage of $|y| < 1$. The axial magnetic field was decreased from the nominal value of 0.5 T to 0.1 T. This greatly improved the efficiency of rejecting low-mass electron pairs from γ conversions and Dalitz decays.

The data were taken with five different triggers, two selecting pions and three selecting electrons. The π triggers required a coincidence between a signal in one of the scintillation counters, positioned behind the Cherenkov counters, and the event time. The latter was defined by the beam–beam counters (not shown in fig. 1) positioned around the beam pipes downstream of the spectrometer, and by the inner-hodoscope counters which surrounded the intersection region at large angle. The first electron trigger, the minimum-bias (MB) trigger, required a coincidence between the event time, a hit in one of the scintillators, and a signal from the corresponding Cherenkov counter. In order to be able to trigger on electrons with higher momentum, the NaI detector was used in the PT trigger. This trigger had the same requirements as the MB trigger and, in addition, a requirement of a minimum energy deposition in the NaI detector, which corresponded to a $p_T > 0.2$ GeV/c. The third electron trigger (the E_{TOT} trigger) used the total energy deposited in the uranium calorimeter together with the requirements of the MB trigger. With this trigger, events with a total energy above a threshold of ~ 8 GeV were selected. A pion trigger with the same requirement on total energy was used together with this electron trigger.

3. DATA TAKING AND RECONSTRUCTION

In this analysis we have used the full event sample available, which consists of 850,000 events recorded with the MB trigger, 1,160,000 events recorded with the PT trigger, and 800,000 events recorded with the E_{TOT} trigger. Most of the events originated from Dalitz decays and photons converting in the beam pipe, the inner hodoscope, or the drift-chamber wall. All of the 2,810,000 events were processed through the AFS track-finding and track-and-vertex fitting programs. At this stage it was required that the events had exactly one track which could be extrapolated to the scintillation counters. Invariant masses of particle pairs were calculated by combining the trigger track with all other reconstructed tracks of opposite charge, assuming both tracks to be electrons. Only events which had no mass combination less than 0.04 GeV/c^2 were kept for further analysis. After this data reduction, the remaining events were processed through the shower reconstruction programs of the NaI detector and the uranium calorimeter.

4. DATA ANALYSIS

The off-line rejection of pions in the electron sample and the rejection of low-mass pairs from γ conversions and Dalitz decays has already been described in our previous publication [1]. The efficiency of the PT trigger was calculated by using a background sample of electrons from converted photons which were triggered by the MB trigger, but where the information from the PT trigger was recorded. Only PT-triggered events where the triggering electron had a $p_T > 0.2$ GeV/c (a trigger efficiency > 50%) were used in this analysis.

The total energy (E_{tot}) in the calorimeter was calculated by summing up all showers with an energy > 0.05 GeV/c, disregarding the showers in the retracted wall. The event sample was divided into four E_{tot} bins and the mean charged multiplicity (including the trigger track) in the rapidity region $|y| < 1$ was calculated. Figure 2 shows the measured charged multiplicity distributions for the four different E_{tot} bins. The efficiency- and acceptance-corrected mean multiplicity was a factor of 1.2 higher than the measured multiplicity according to Monte Carlo calculations. In this energy domain jets are not dominating and the mean charged multiplicity is proportional to E_{tot}.

The division into E_{tot} bins rather than multiplicity bins was necessary in order to avoid a trivial distortion of the measured e^+/π ratio versus multiplicity. If the triggering positrons originated from a pair source, the multiplicity distribution for these events, compared with the distribution from pion-triggered events, was shifted to higher values owing to the second electron in the pair and this introduced a form of trigger bias when the sample was divided up into multiplicity bins.

In the final analysis it was required that the electron-trigger track did not combine with any track of opposite sign to form a pair with an invariant mass < 0.1 GeV/c^2. The efficiency of this cut was strongly depending on the multiplicity, and therefore this efficiency had to be calculated separately for each E_{tot} bin (see fig. 3). This was the only efficiency correction that was different for different E_{tot} bins since all other cut efficiencies were either independent of E_{tot} or were the same for electrons and pions.

The residual background from γ conversions and Dalitz decays was calculated with a Monte-Carlo simulation program as described in ref. [1], and subtracted from the measured e^+/π. Only triggering positrons were used since the electron sample had a large contamination of electrons coming from Compton scattering. It was assumed that the residual e^+/π background was independent of E_{tot}, as confirmed in section 5 below.

5. RESULTS

The event sample in each E_{tot} bin was subdivided into three p_T bins. Figure 4 shows the e^+/π ratio after background subtraction and efficiency corrections versus mean E_{tot} for the three different p_T bins. A striking difference is observed for the E_{tot} dependence of the e^+/π ratio in the different p_T intervals. In the highest p_T bin there seems to be no significant rise of the e^+/π ratio as E_{tot} increases, while the confidence levels (CLs) for a constant value of e^+/π in the two lowest p_T bins are only 5% and 2%, and with the two bins combined the CL is as low as 0.7%. The lines in fig. 4 show linear least squares fits to the data with the resulting parameters given in table 1.

The results in fig. 4 are the weighted average of measurements done with data taken with the three different electron triggers. As can be seen in table 2, all three data samples were consistent and showed the same increase of the e^+/π ratio with E_{tot} at low p_T. From this we could conclude that there was no obvious trigger bias.

Since the result depends strongly on the efficiency corrections for the mass cut, the analysis was redone with a mass cut at 0.05 GeV/c^2. With this mass cut the efficiency corrections were much smaller (see fig. 3) and the result was not so sensitive to these corrections. We found the same strong E_{tot} dependence with the lower mass cut at 0.05 GeV/c^2 as with the higher mass cut at 0.1 GeV/c^2, and this assured us that there was not a large systematic error in our efficiency calculations.

Finally, the same analysis was done with zero-mass electron pairs that originated from the large background sample of γ's converting before the drift chamber. This measurement of e^+/π is presented in fig. 5. No significant rise is seen in this e^+/π ratio with increasing E_{tot}. From this measurement we conclude that the division of our sample into E_{tot} bins does not introduce a biased selection of low-p_T triggers with high multiplicity and that the background from photons relative to the number of pions does not increase significantly with multiplicity.

6. DISCUSSION

The main known sources contributing to the measured e^+/π ratio in the p_T region $0.12 < p_T < 1.0$ GeV/c are hadronic bremsstrahlung and semileptonic decay of charmed particles. Both sources are expected to increase linearly with the multiplicity, thus giving a constant contribution to the measured e^+/π ratio. Indeed, we see that in the p_T region of 0.4–1.0 GeV/c, where charm is supposed to be the dominating source of positrons, little or no dependence of the e^+/π ratio on E_{tot} is observed. However, in the p_T region below 0.4 GeV/c, where we previously [1] have seen an excess of positrons above known sources, the e^+/π ratio increases linearly with E_{tot}, i.e. the e^+ production increases with the square of the total energy, which is equivalent to the mean charged multiplicity.

A number of experiments have reported observations of a lepton-pair continuum with masses $m < 0.6$ GeV/c^2, i.e. below the ϱ^0 and ω. It has recently been pointed out [9] that information about the production mechanism of the low-mass e^+e^- continuum can be obtained by studying the associated charged multiplicity in a rapidity region close to that of the lepton pairs. If the dileptons are created after the final hadrons have been produced (i.e. by hadron decays or hadronic bremsstrahlung), the mean number of dileptons per event will be proportional to the number of final hadrons, thus giving a constant value of the e^+/π ratio. In another class of models, the lepton pairs are produced over an extended volume at an early time during the collision when new quarks and antiquarks have been created and the lepton production is enhanced by including interactions between the many quarks and antiquarks **produced** in the hadron–hadron collision. The production rate of dileptons in these models should be proportional to the density of quarks times the density of antiquarks, i.e. proportional to the square of the charged-particle multiplicity. This characteristic dependence is predicted by the soft-annihilation model [9] and the thermodynamic models [11].

It has been suggested that the phase transition between hadronic matter and quark matter in very high energy nucleus–nucleus collisions could be detectable by measuring the production rate of lepton pairs [13]. Amongst other features, a square dependence of this rate on particle multiplicity is predicted as one of the signatures for the quark–gluon plasma [11]. As we find the same characteristic increase of the e^+/π ratio already in pp collisions, it must be in the quantitative analysis of the lepton-pair production in ultrarelativistic nuclear collisions that new effects should be sought.

In conclusion, we find that the production of low-p_T positrons ($p_T < 0.4$ GeV/c) increases as a function of the square of the total energy measured in the calorimeter, which is proportional to the mean charged multiplicity in the rapidity region $|y| < 1$. This excludes hadronic bremsstrahlung and the decay of charmed particles as an explanation for the observed e^+/π ratio, but it is in a good agreement with the predictions of the soft-annihilation model and the thermodynamic models.

7. ACKNOWLEDGEMENTS

We thank CERN for the loan of the Cherenkov counters from the R607 experiment at the ISR. We are also grateful to the emulator group at the CERN DD Division who made it possible to process three million events. Support from the Research Councils in our home countries and from the Experimental Support Group of the ISR is gratefully acknowledged.

REFERENCES

[1] T. Åkesson et al., Phys. Lett. **152B** (1985) 411.

[2] L. Baum et al., Phys. Lett. **60B** (1976) 485;
M. Barone et al., Nucl. Phys. **B132** (1978) 29;
M. Heiden, Ph.D. Thesis, CERN EP Internal Report 82-05 (1982).

[3] E.W. Beier et al., Phys. Rev. Lett. **37** (1976) 1117;
A. Maki et al., Phys. Lett. **106B** (1981) 423.

[4] Y. Makdisi et al., Phys. Rev. Lett. **41** (1978) 367;
R. Barloutaud et al., Nucl. Phys. **B172** (1980) 25.

[5] M.R. Adams et al., Phys. Rev. **D27** (1983) 1977;
D. Blockus et al., Nucl. Phys. **B201** (1982) 205;
S. Mikamo et al., Phys. Lett. **106B** (1981) 428;
J. Ballam et al., Phys. Rev. Lett. **41** (1978) 1207.

[6] K.J. Anderson et al., Phys. Rev. Lett. **37** (1976) 799;
K. Bunnell et al., Phys. Rev. Lett. **40** (1978) 136;
B. Haber et al., Phys. Rev. Lett. **D22** (1980) 2107;
J. Alspector et al., Phys. Lett. **81B** (1979) 397;
R.I. Dzhelyadin et al., Nucl. Phys. **B179** (1981) 189;
M. Faessler et al., Phys. Rev. **D17** (1978) 689;
W.M. Morse et al., Phys. Rev. **D18** (1978) 3145.

[7] V. Cerny et al., Phys. Rev. **D24** (1981) 652;
V. Cerny et al., Acta Phys. Pol. **B10** (1979) 537;
V. Cerny et al., Acta Phys. Pol. **B9** (1978) 901.

[8] J.D. Bjorken and H. Weisberg, Phys. Rev. **D13** (1976) 1405.

[9] V. Cerny, P. Lichard and J. Pisut, Z. Phys. C. **31** (1986) 163.

[10] E.V. Shuryak, Phys. Rep. **61** (1980) 71;
T. Adachi and I. Yotsuyanagi, Phys. Rev. **D23** (1981) 1106;
E.V. Shuryak, CERN 83-01 (1983).

[11] R.C. Hwa and K. Kajantie, Phys. Rev. **D32** (1985) 1109.

[12] T. Åkesson et al., Nucl. Instrum. Methods **196** (1982) 303, 315;
O. Botner et al., Nucl. Instrum. Methods **196** (1982) 315;
R. Batley et al., Nucl. Instrum. Methods **A242** (1985) 75;
T. Åkesson et al., Nucl. Instrum. Methods **A241** (1985) 17.

[13] E.V. Shuryak, Sov. J. Nucl. Phys. **28** (1978) 408;
G. Domokos and J.I. Goldman, Phys. Rev. **D23** (1981) 203;
L.D. McLerran and T. Toimela, Phys. Rev. **D31** (1985) 545;
K. Kajantie and H.I. Miettinen, Z. Phys. C. **9** (1981) 341;
K. Kajantie et al., Helsinki University preprint HU-TFT-86-6 (1986).

Table 1

Fit to the function $e^+/\pi = (A + B \cdot E_{tot}) \times 10^{-4}$

p_T (GeV/c)	A	B	χ^2	N.D.F.[a)]
$0.12 < p_T < 0.20$	-1.7 ± 4.3	1.6 ± 0.6	0.70	2
$0.20 < p_T < 0.40$	1.2 ± 1.1	0.50 ± 0.18	1.78	2
$0.40 < p_T < 1.00$	1.6 ± 0.7	0.12 ± 0.10	2.31	2

a) Number of degrees of freedom.

Table 2

The residual e^+/π ratio for different triggers
(The values within the parenthesis were not used in the weighted average since the trigger efficiency was < 50%)

E_{tot} bin (GeV)	p_T bin (GeV/c)	MB trigger $(e^+/\pi) \times 10^4$	PT trigger $(e^+/\pi) \times 10^4$	E_{TOT} trigger $(e^+/\pi) \times 10^4$	$\langle E_{tot} \rangle$ (GeV)	Weighted average $\langle p_T \rangle$ (MeV/c)	$\langle n \rangle$	$(e^+/\pi) \times 10^4$
$2 < E_{tot} < 5$	$0.12 < p_T < 0.2$	3.84 ± 2.70	(3.65 ± 2.12)		3.9	152	5.0	3.84 ± 2.70
$5 < E_{tot} < 8$	$0.12 < p_T < 0.2$	10.85 ± 3.37	(10.96 ± 2.27)		6.3	158	7.8	10.85 ± 3.37
$8 < E_{tot} < 11$	$0.12 < p_T < 0.2$	8.77 ± 6.49	(14.91 ± 4.33)	16.75 ± 4.64	9.3	157	11.5	14.05 ± 3.77
$11 < E_{tot} < 18$	$0.12 < p_T < 0.2$		(25.63 ± 11.44)	17.27 ± 5.54	12.9	156	14.2	17.27 ± 5.54
$2 < E_{tot} < 5$	$0.2 < p_T < 0.4$	3.40 ± 1.29	3.59 ± 0.76		3.9	283	5.0	3.54 ± 0.65
$5 < E_{tot} < 8$	$0.2 < p_T < 0.4$	5.15 ± 1.57	3.51 ± 0.62		6.3	282	7.8	3.73 ± 0.58
$8 < E_{tot} < 11$	$0.2 < p_T < 0.4$	8.23 ± 3.49	5.07 ± 1.28	8.07 ± 2.11	9.3	281	11.5	6.09 ± 1.04
$11 < E_{tot} < 18$	$0.2 < p_T < 0.4$		10.58 ± 3.69	7.82 ± 2.50	12.9	296	14.2	8.69 ± 2.07
$2 < E_{tot} < 5$	$0.4 < p_T < 1.0$	1.74 ± 0.93	2.35 ± 0.49		3.9	679	5.0	2.22 ± 0.43
$5 < E_{tot} < 8$	$0.4 < p_T < 1.0$	1.33 ± 0.87	2.16 ± 0.41		6.3	701	7.8	2.01 ± 0.37
$8 < E_{tot} < 11$	$0.4 < p_T < 1.0$	10.73 ± 3.17	3.44 ± 0.78	2.34 ± 1.11	9.3	714	11.5	3.37 ± 0.63
$11 < E_{tot} < 18$	$0.4 < p_T < 1.0$		2.78 ± 1.47	2.61 ± 1.21	12.9	740	14.2	2.68 ± 0.93

Figure captions

Fig. 1 Experimental set-up.

Fig. 2 Multiplicity distributions for the four different E_{tot} bins.

Fig. 3 The efficiency for a mass cut at a) 100 MeV/c^2 and b) 50 MeV/c^2. This efficiency was calculated by using the pion sample.

Fig. 4 The residual e^+/π ratio after background subtraction as a function of total energy, measured with the uranium calorimeter. The top scale indicates the mean charged multiplicity which corresponds to the measured E_{tot}.

Fig. 5 The e^+/π ratio as a function of E_{tot} (and the corresponding multiplicity) where the electron originates from a γ which had converted before the drift chamber.

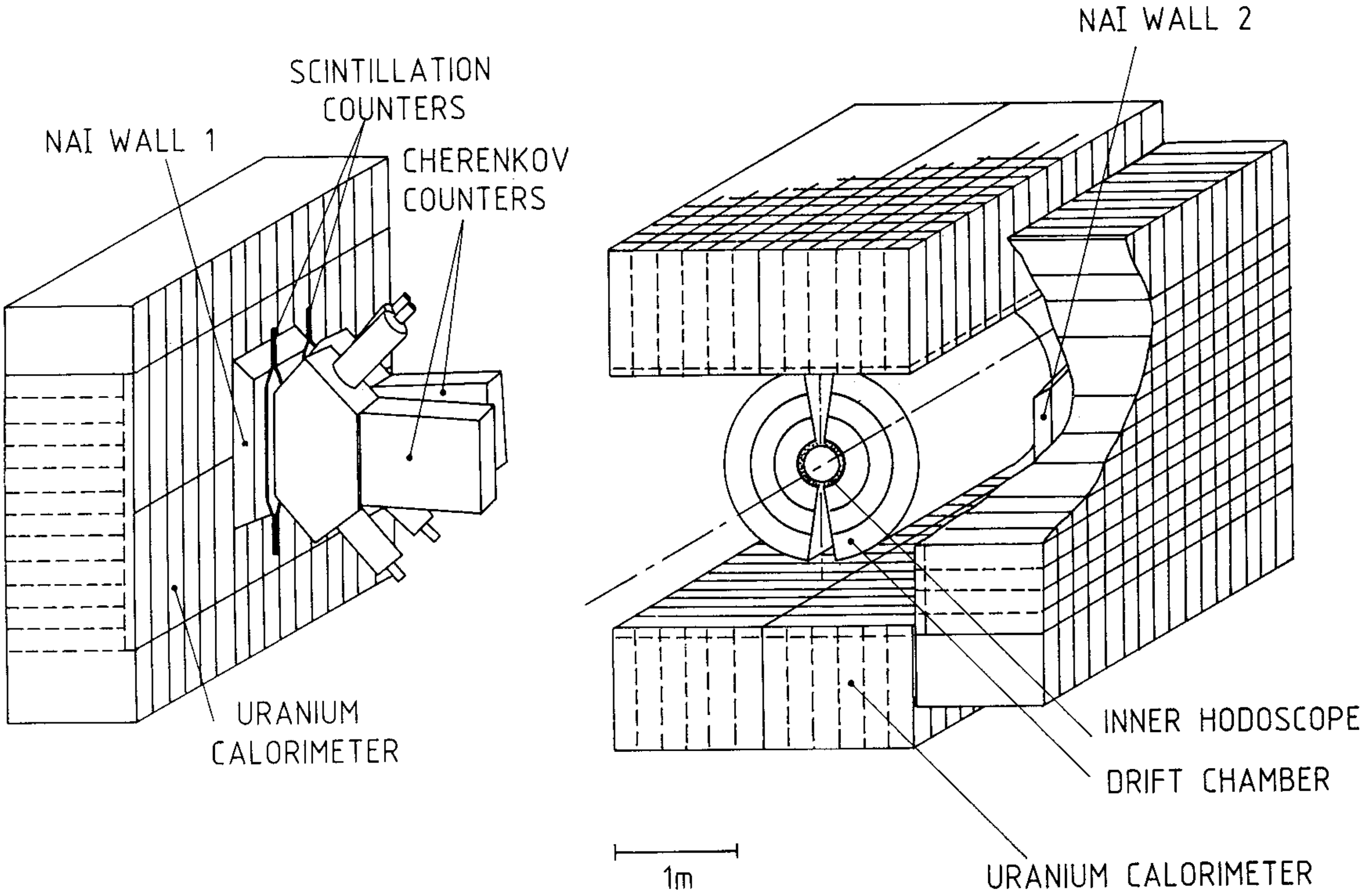
NAI WALL 1
SCINTILLATION COUNTERS
CHERENKOV COUNTERS
URANIUM CALORIMETER
NAI WALL 2
INNER HODOSCOPE
DRIFT CHAMBER
URANIUM CALORIMETER
1m

Fig. 1

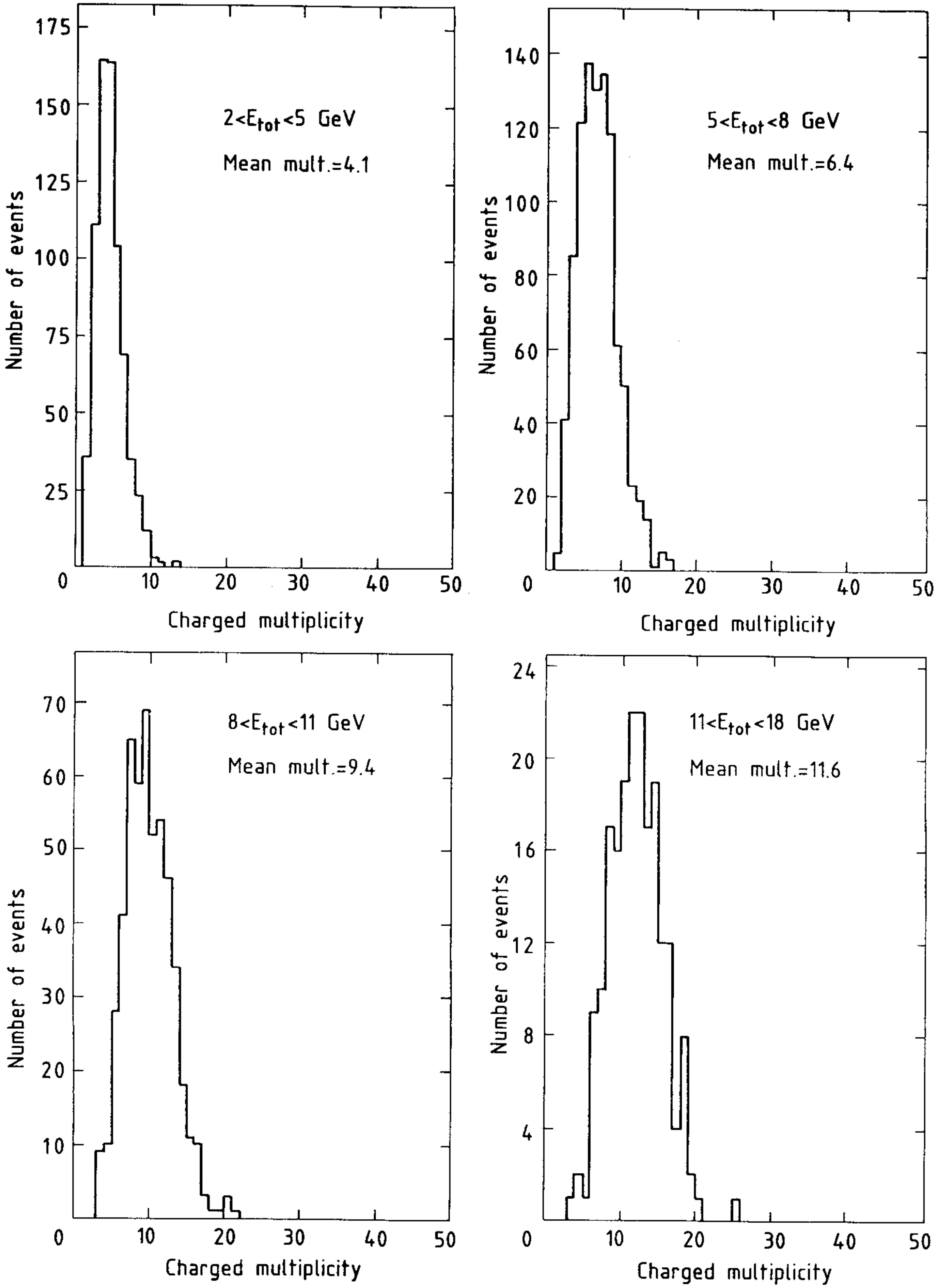
2<E_tot<5 GeV
Mean mult.=4.1
5<E_tot<8 GeV
Mean mult.=6.4
8<E_tot<11 GeV
Mean mult.=9.4
11<E_tot<18 GeV
Mean mult.=11.6
Number of events
Charged multiplicity
0
10
20
30
40
50

Fig. 2

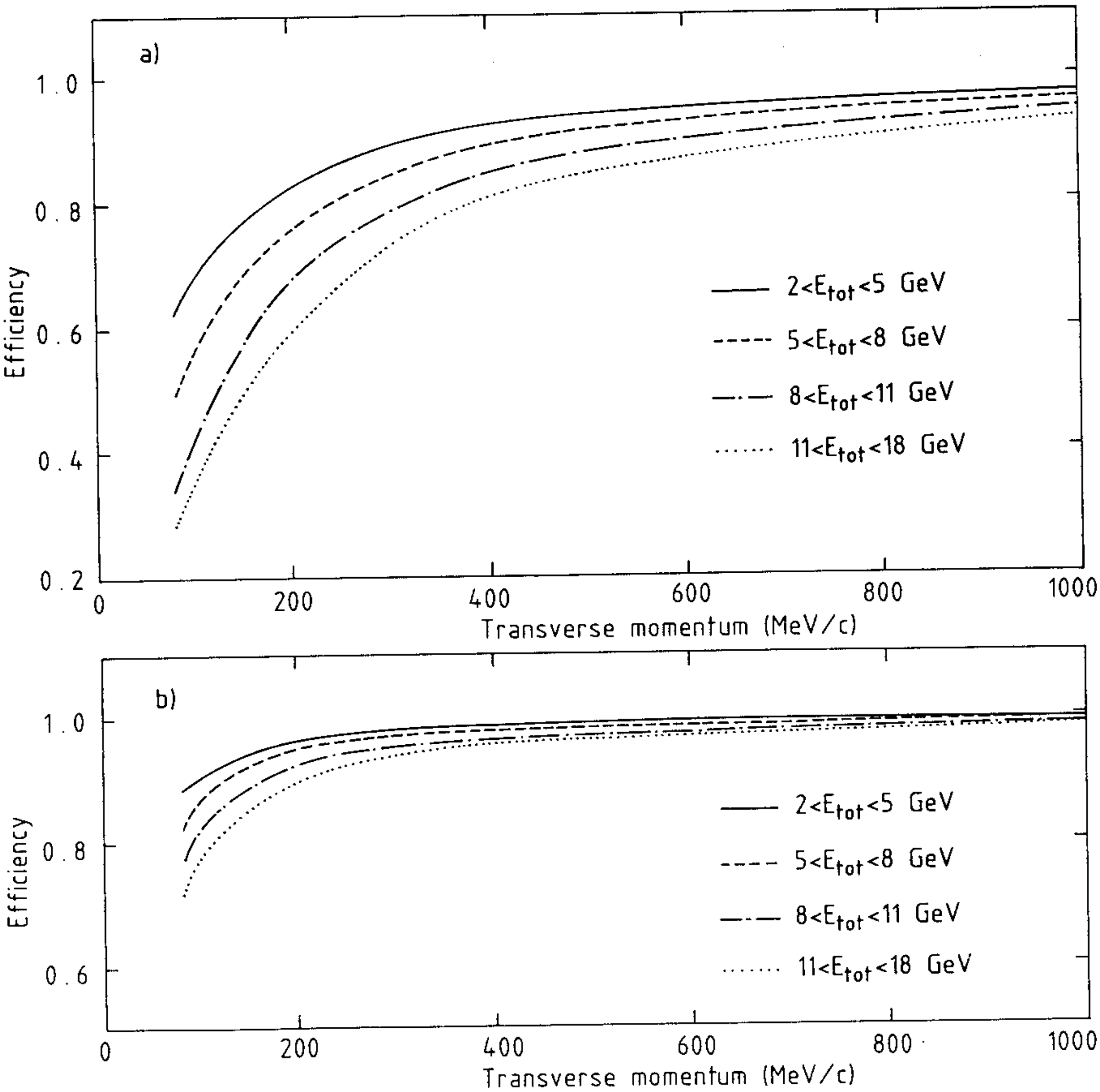

a)
b)
Efficiency
Transverse momentum (MeV/c)
0.2
0.4
0.6
0.8
1.0
0
200
400
600
800
1000
2<E_tot<5 GeV
5<E_tot<8 GeV
8<E_tot<11 GeV
11<E_tot<18 GeV

Fig. 3

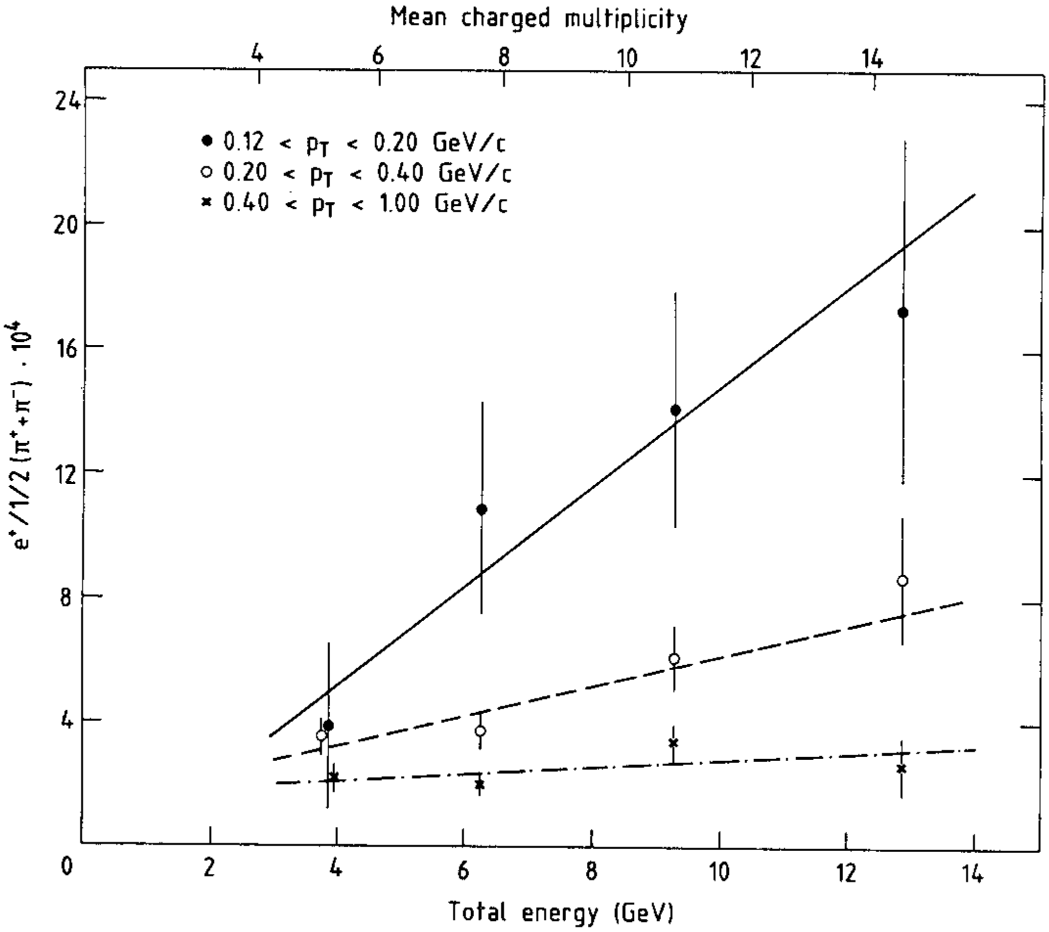
Mean charged multiplicity
4
6
8
10
12
14
24
20
16
12
8
4
0
● 0.12 < pT < 0.20 GeV/c
○ 0.20 < pT < 0.40 GeV/c
× 0.40 < pT < 1.00 GeV/c
e+/1/2 (π+ + π−) · 10^4
2
4
6
8
10
12
14
Total energy (GeV)

Fig. 4

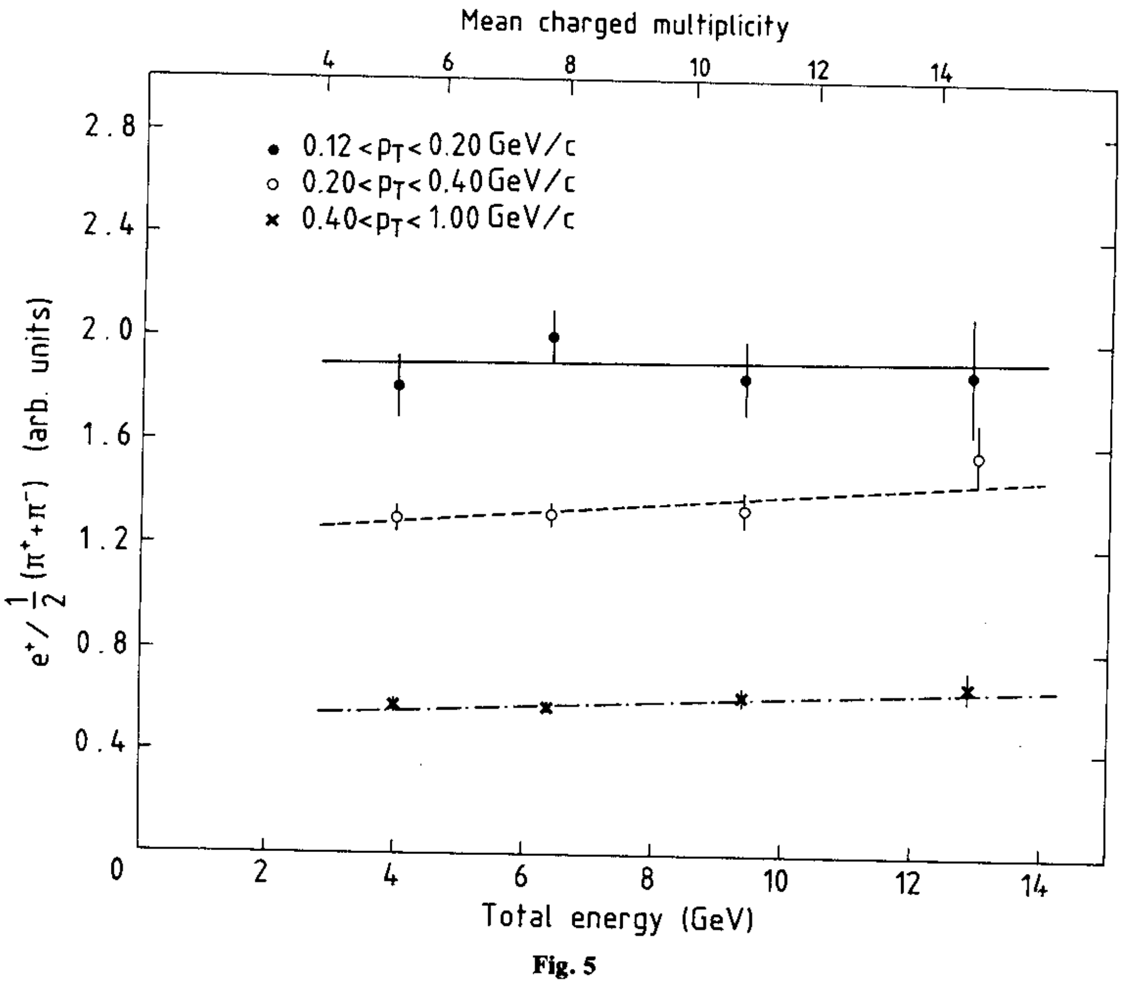
Mean charged multiplicity
4
6
8
10
12
14
2.8
2.4
2.0
1.6
1.2
0.8
0.4
0
● 0.12<pT<0.20 GeV/c
○ 0.20<pT<0.40 GeV/c
× 0.40<pT<1.00 GeV/c
e+/ 1/2 (π+ + π−) (arb. units)
2
4
6
8
10
12
14
Total energy (GeV)

Fig. 5